論文 한국정밀공학회지 제 12 권 제 1 호 1995. 1
Journal of the Korean Society of Precision Engineering Vol. 12. No 1. January. 1995.

수치해석을 통한 자기보상 동적균형기의 작동성 검토

이 종 길*

Numerical Simulation of Self-Compensating Dynamic Balancer in a Rotating Mechanism

Jongkil Lee*

ABSTRACT

회전체의 자동밸런싱을 위하여 고안된 자기보상 동적균형기는 홈이파인 원판에 강구와 저점성유체를 지닌 구조체이다. 유도된 운동방정식으로 부터 자기보상 동적균형기의 작동조건을 조사하기 위하여 수치해석을 통한 동특성을 검토하였다. 수치해석의 결과에 근거하여 임계속도보다 높은 범위에서는 자기보상 동적균형기는 정상작동을 보여주었다. 임계속도에서는 회전계의 균형이 강구와 점성유체와의 감쇠계수에 의존하였으나 임계속도보다 낮은 범위에서는 어떠한 조건에 대해서도 작동하지 않음을 알 수 있었다. 자동차 및 항공기에도 응용가능한 자기보상 동적균형기의 작동조건들을 본 논문에서 예시하였다.

Key Words : Self-Compensating Dynamic Balancer(자기보상동적균형기), Numerical Simulation(수치해석), Rotating Machinery(회전기계), Critical Speed(임계속도), Normalized Displacement(무차원변위)

1. Introduction

The unbalance in the rotors of rotating machinery causes vibrations and generates undesirable forces. These forces are transmitted to the machine parts and it may cause damage to the whole system. Generally, this unbalance is a result of unavoidable imperfections in rotor manufacture and assembly. Therefore, the balancing of rotors is clearly important and is accepted as a fundamental requirement for the normal operation of modern low and high speed rotating machines.

The idea of an automatic dynamic balancer, or Self-Compensating Dynamic Balancer (SCDB), has been proposed, in many forms and applications, through numerous patents to eliminate the need for balancing and yet minimize the effects of rotor unbalance and vibratory forces on the rotating system during normal operation. The automatic dynamic balancer is usually composed of a circular disk

* 국방과학연구소

with a groove, or race, containing spherical or cylindrical weights and a low viscosity damping fluid, although early attempts used other approaches. This idea is claimed to be applicable for many applications, ranging from space vehicle components, to washing machines. The purpose of this paper is to develop a numerical understanding of the motion of the weights in SCDB and how this limits the operation.

2. Mathematical Model for Numerical Simulation

A rotating unbalanced disk with a SCDB and supported by springs is shown in Fig. 1. The rotating disk is of mass M and the SCDB balls are each of mass m. The point C represents the deflected centerline of the rotating system, and the point G represents the location of the mass center of the disk, not including the SCDB balls. Because of imperfections in the disk, its mass center G is located a distance ε from the disk's geometric center at C. Assume that the center C of the disk is located at the origin O of the XYZ axes when the supporting springs are undeflected. The equations of motion of this system can be derived by the Lagrangian

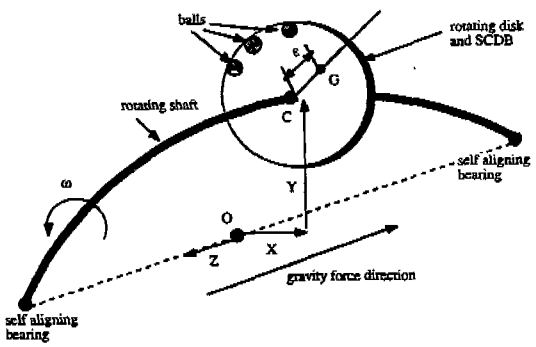

Fig. 1 Rotating system of the SCDB

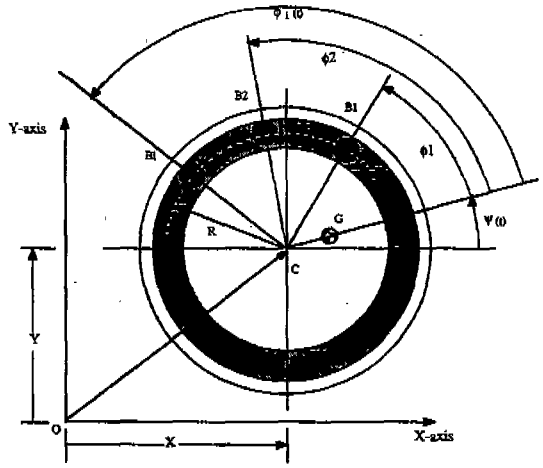

Fig. 2 Self-Compensating Dynamic Balancer

method. For a circular shaft it is logical to assume that the stiffness, k, and the damping of the shaft, c, are the same regardless of the orientation of the shaft. Therefore, a scalar Lagrangian function, L, is

$$L = \frac{1}{2}I_z\dot{\psi}^2 + \frac{1}{2}M\left[\dot{X}^2 + \dot{Y}^2 - 2\varepsilon\dot{\psi}\dot{X}\sin\psi + \varepsilon^2\dot{\psi}^2 + 2\varepsilon\dot{\psi}\dot{Y}\cos\psi\right] + \frac{1}{2}\sum_{i=1}^{n}\left(m_i + \frac{2}{5}m_i\right)\left\{\dot{X}^2 + \dot{Y}^2 + \left(\dot{\phi}_i + \dot{\psi}\right)^2 R^2 - 2R\left(\dot{\phi}_i + \dot{\psi}\right)\left[\dot{X}\sin\left(\phi_i + \psi\right) - \dot{Y}\cos\left(\phi_i + \psi\right)\right]\right\} - \frac{1}{2}k\left(X^2 + Y^2\right) \quad (1)$$

where, gravitational effects have been ignored. Iz is mass moment of inertia of the disk. If the angular velocity of the disk is constant, then $\ddot{\psi} = 0, \dot{\psi} = \omega$ and $\Psi = \omega t$ where, ω is a rotation speed of the shaft. The euqations of motion for the shaft and the two balls are

$$\left[1 + n\left(\frac{m}{M}\right)\right]\frac{\ddot{X}}{\omega_n{}^2 R} + \frac{2\zeta}{\omega_n}\frac{\dot{X}}{R} + \frac{X}{R} - \frac{\varepsilon}{R}\left(\frac{\omega}{\omega_n}\right)^2$$

$$\cos(\omega t) - \frac{1}{\omega_n^2}\frac{m}{M}\Big[\ddot{\phi}_1 \sin(\phi_1 + \omega t) + (\dot{\phi}_1 + \omega)^2 \cos(\phi_1 + \omega t) + \ddot{\phi}_2 \sin(\phi_2 + \omega t) + (\dot{\phi}_2 + \omega)^2 \cos(\phi_2 + \omega t)\Big] = 0, \quad (2a)$$

$$\left[1 + n\left(\frac{m}{M}\right)\right]\frac{\ddot{Y}}{\omega_n^2 R} + \frac{2\zeta}{\omega_n}\frac{\dot{Y}}{R} + \frac{Y}{R} - \frac{\varepsilon}{R}\left(\frac{\omega}{\omega_n}\right)^2 \sin(\omega t) + \frac{1}{\omega_n^2}\frac{m}{M}\Big[\ddot{\phi}_1 \cos(\phi_1 + \omega t) - (\dot{\phi}_1 + \omega)^2 \sin(\phi_1 + \omega t) + \ddot{\phi}_2 \cos(\phi_2 + \omega t) - (\dot{\phi}_2 + \omega)^2 \sin(\phi_2 + \omega t)\Big] = 0, \quad (2b)$$

$$\frac{\ddot{\phi}_1}{\omega_n^2} - \frac{1}{\omega_n^2}\frac{\ddot{X}}{R}\sin(\phi_1 + \omega t) + \frac{1}{\omega_n^2}\frac{\ddot{Y}}{R}\cos(\phi_1 + \omega t) + \frac{1}{R\omega_n^2}(\dot{\phi}_1 + \omega)\Big[\dot{X}\cos(\phi_1 + \omega t) + \dot{Y}\sin(\phi_1 + \omega t)\Big] = -\beta\frac{\dot{\phi}_1}{\omega_n^2}, \quad (2c)$$

and

$$\frac{\ddot{\phi}_2}{\omega_n^2} - \frac{1}{\omega_n^2}\frac{\ddot{X}}{R}\sin(\phi_2 + \omega t) + \frac{1}{\omega_n^2}\frac{\ddot{Y}}{R}\cos(\phi_2 + \omega t) + \frac{1}{R\omega_n^2}(\dot{\phi}_2 + \omega)\Big[\dot{X}\cos(\phi_2 + \omega t) + \dot{Y}\sin(\phi_2 + \omega t)\Big] = -\beta\frac{\dot{\phi}_2}{\omega_n^2}. \quad (2d)$$

When a differential equation cannot be integrated in closed form, numerical methods must be employed. This may well be the case when the system is nonlinear or if the system is excited by a force that cannot be expressed by simple analytic functions. Consider the rotating system consisted of a single SCDB, which has two steel balls, mounted on the midspan of rotating shaft. If we assume the shaft rotates at constant speed, regardless of what method may be used to numerically integrate the equations, the first step is to transform the given second order equations, (2), to a system of first order equations. To develop a procedure which can be easily used for a computer solution, let

$$\begin{bmatrix} y_1 \\ y_2 \\ y_3 \\ y_4 \\ y_5 \\ y_6 \\ y_7 \\ y_8 \end{bmatrix} = \begin{bmatrix} X \\ \dot{X} \\ Y \\ \dot{Y} \\ \phi_1 \\ \dot{\phi}_1 \\ \phi_2 \\ \dot{\phi}_2 \end{bmatrix}, \quad (3a)$$

the velocities are obtained as

$$\begin{bmatrix} \frac{dy_1}{dt} \\ \frac{dy_3}{dt} \\ \frac{dy_5}{dt} \\ \frac{dy_7}{dt} \end{bmatrix} = \begin{bmatrix} y_2 \\ y_4 \\ y_6 \\ y_8 \end{bmatrix}, \quad (3b)$$

and the accelerations are obtained as

$$\begin{bmatrix} \frac{dy_2}{dt} \\ \frac{dy_4}{dt} \\ \frac{dy_6}{dt} \\ \frac{dy_8}{dt} \end{bmatrix} = \begin{bmatrix} \ddot{X} \\ \ddot{Y} \\ \ddot{\phi}_1 \\ \ddot{\phi}_2 \end{bmatrix}. \quad (3c)$$

Second order equations, (2), can be transformed into a system of first order equations and then solved using the Runge-Kutta method. It can be seen that $\frac{dy_2}{dt}, \frac{dy_4}{dt}, \frac{dy_6}{dt}$, and $\frac{dy_8}{dt}$ can be obtained by transforming the original differential equations, (2), into four simultaneous first order differential equations using equation (3). It is convenient to express

the equations (2) using matrix form as

$$[A]\begin{bmatrix}\frac{dy_2}{dt}\\ \frac{dy_4}{dt}\\ \frac{dy_6}{dt}\\ \frac{dy_8}{dt}\end{bmatrix}=\begin{bmatrix}f_{11}\\ f_{21}\\ f_{31}\\ f_{41}\end{bmatrix} \tag{4a}$$

where,

$$[A]=\begin{bmatrix}a_{11} & 0 & a_{13} & a_{14}\\ 0 & a_{22} & a_{23} & a_{24}\\ a_{31} & a_{32} & 1 & 0\\ a_{41} & a_{42} & 0 & 1\end{bmatrix}$$

$$=\begin{bmatrix}\frac{1+n\left(\frac{m}{M}\right)}{\omega_n{}^2R} & 0 & -1\frac{1}{\omega_n{}^2}\frac{m}{M}(y_5+\omega t) & -\frac{1}{\omega_n{}^2}\frac{m}{M}\sin(y_7+\omega t)\\ 0 & \frac{1+n\left(\frac{m}{M}\right)}{\omega_n{}^2R} & \frac{1}{\omega_n{}^2}\frac{m}{M}\cos(y_5+\omega t) & \frac{1}{\omega_n{}^2}\frac{m}{M}\cos(y_7+\omega t)\\ -\frac{\sin(y_5+\omega t)}{\omega_n{}^2R} & \frac{\cos(y_5+\omega t)}{\omega_n{}^2R} & 1 & 0\\ -\frac{\sin(y_7+\omega t)}{\omega_n{}^2R} & \frac{\cos(y_7+\omega t)}{\omega_n{}^2R} & 0 & 1\end{bmatrix}, \tag{4b}$$

$$f_{11}=-\frac{2\zeta}{\omega_n}\frac{y_2}{R}-\frac{y_1}{R}+\frac{\varepsilon}{R}\left(\frac{\omega}{\omega_n}\right)^2\cos(\omega t)+\frac{1}{\omega_n{}^2}\frac{m}{M}\left[(y_6+\omega)^2\cos(y_5+\omega t)+(y_8+\omega)^2\cos(y_7+\omega t)\right], \tag{4c}$$

$$f_{21}=-\frac{2\zeta}{\omega_n}\frac{y_4}{R}-\frac{y_3}{R}+\frac{\varepsilon}{R}\left(\frac{\omega}{\omega_n}\right)^2\sin(\omega t)+\frac{1}{\omega_n{}^2}\frac{m}{M}\left[(y_6+\omega)^2\sin(y_5+\omega t)+(y_8+\omega)^2\sin(y_7+\omega t)\right], \tag{4d}$$

$$f_{31}=-\frac{1}{R\omega_n{}^2}(y_6+\omega)\left[y_2\cos(y_5+\omega t)+y_4\sin(y_5+\omega t)\right]-\beta\frac{y_6}{\omega_n{}^2}, \tag{4e}$$

and

$$f_{41}=-\frac{1}{R\omega_n{}^2}(y_8+\omega)\left[y_2\cos(y_7+\omega t)+y_4\sin(y_7+\omega t)\right]-\beta\frac{y_8}{\omega_n{}^2}, \tag{4f}$$

Therefore, these four derivatives can be obtained as

$$\frac{dy_2}{dt}=-(a_{13}a_{32}f_{21}+a_{23}a_{32}f_{11}+a_{13}a_{32}a_{24}f_{41}+a_{14}a_{42}a_{23}f_{31}-a_{11}f_{11}+a_{11}a_{13}f_{31}+a_{11}a_{14}f_{41}+a_{24}a_{42}f_{11}-a_{14}a_{42}f_{21}-a_{24}a_{42}a_{13}f_{31}-a_{23}a_{32}a_{14}f_{41})/\Delta, \tag{5a}$$

$$\frac{dy_4}{dt}=-(a_{13}a_{31}f_{21}-a_{13}a_{31}a_{24}f_{41}+a_{13}f_{31}a_{24}a_{41}-f_{31}a_{23}a_{14}a_{41}+a_{31}a_{23}a_{14}f_{41}-a_{11}f_{21}+a_{14}a_{41}f_{21}-f_{11}a_{24}a_{41}+a_{11}a_{24}f_{41}+f_{31}a_{23}a_{11}-a_{31}a_{23}f_{11})/\Delta, \tag{5b}$$

$$\frac{dy_6}{dt}=(-a_{42}a_{11}f_{21}-a_{41}a_{11}f_{11}+f_{41}a_{11}{}^2-a_{41}a_{13}a_{32}f_{21}+a_{41}a_{23}a_{32}f_{11}+a_{41}a_{11}a_{13}f_{31}+a_{42}a_{13}a_{31}f_{21}+a_{42}f_{31}a_{23}a_{11}-a_{42}a_{31}a_{23}f_{11}-f_{41}a_{11}a_{13}a_{31})/\Delta, \tag{5c}$$

$$\frac{dy_8}{dt}=(-a_{31}a_{11}f_{11}+a_{14}a_{41}a_{32}f_{21}-a_{11}a_{32}f_{21}-a_{31}a_{14}a_{42}f_{21}-f_{11}a_{32}a_{24}a_{41}+a_{11}a_{32}a_{24}f_{41}+f_{31}a_{11}{}^2+a_{31}a_{11}a_{14}f_{41}+a_{31}a_{24}a_{42}f_{11}-f_{31}a_{24}a_{42}a_{11}-f_{31}a_{11}a_{14}a_{41})/\Delta, \tag{5d}$$

and

$$\Delta=a_{11}{}^2-a_{23}a_{32}a_{11}-a_{13}a_{32}a_{24}a_{41}-a_{14}a_{42}a_{23}a_{31}-a_{24}a_{42}a_{11}+a_{24}a_{42}a_{13}a_{31}+a_{23}a_{32}a_{14}a_{41}-a_{11}a_{14}a_{41}-a_{11}a_{13}a_{31}. \tag{5e}$$

These four equations, (5), plus the equations (3b) give a set of first order euqations

describing the system. The Runge-Kutta computation procedure is popular since it is self-starting and results in good accuracy. To obtain a numerical solution, the mathematical model, (5) plus (3b), is programmed on a digital computer using FORTRAN program language. To numerically model the system parameters must assigned numerical values. The values chosen are

$$\frac{m}{M}=.005,\ \frac{\varepsilon}{R}=.001,\ and\ \beta=2(or\ 5) \qquad (6a)$$

with initial ball positions: 57° and 115°
(or 174° and 186°) (6b)

The initial positions of the balls should have no influence on the final solution, but in numerical simulations these are necessary.

3. Operating above Critical Speed

Fig. 3 to 6 show the results of a computer simulation with two balls. Fig. 3 and 5 show the normalized displacement, X/R, of the system with two balls. These plot show a rapid reduction in unbalance excursions with time and no imbalance after the transient decays. Fig. 4 and Fig. 6 show angular positions, ϕ_1 ($=y_5$) and ϕ_2 ($=y_7$), of the two balls as a function of time. These plots illustrate that

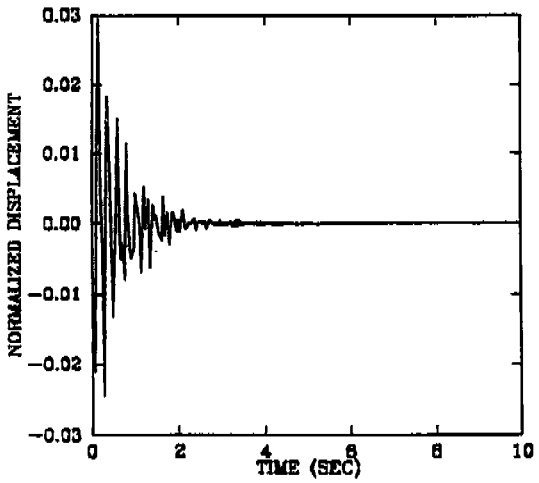

Fig. 3 Normalized displacement of the rotating system above the first critical speed (Run conditions: m/M = .005, ε/R=.001, β=2, and ω/ω_n=1.5)

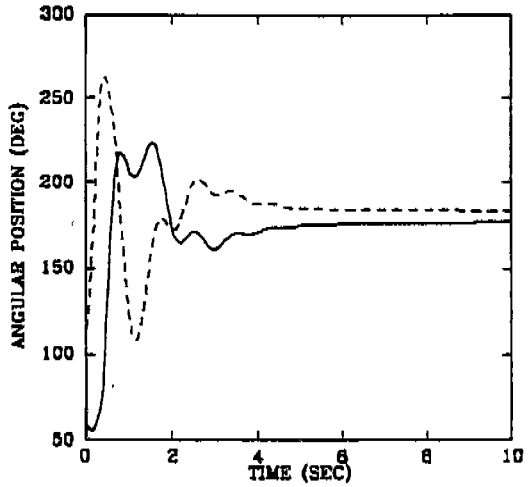

Fig. 4 Angular position of the two balls above the first critical speed (Run conditions: m/M = .005, ε/R=.001, β=2, $\phi_1(0)$=57, $\phi_2(0)$=115, and ω/ω_n=1.5)

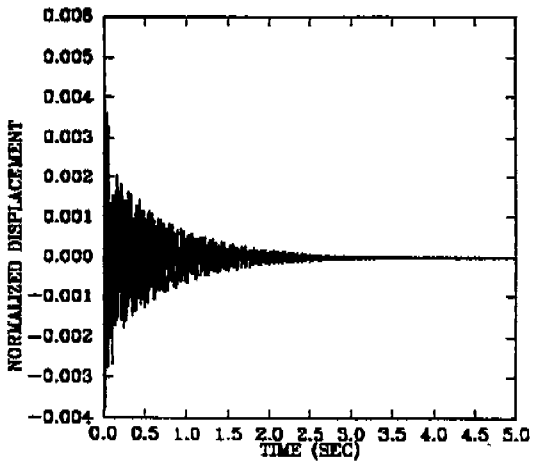

Fig. 5 Normalized displacement of the rotating system above the first critical speed (Run conditions: m/M = .005, ε/R = .001, β = 2, and ω/ω_n= 2)

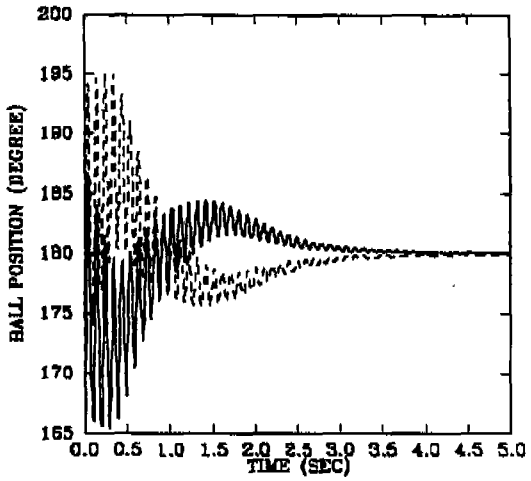

Fig. 6 Angular position of the two balls above the first critical speed (Runconditions: m/M = .005, ϵ/R=.001, β =2, $\phi_1(0)$=57, $\phi_2(0)$=115, and ω/ω_n=2)

when the rotating system is balanced the two balls are approximately positioned at 180 degrees (on the opposite side of the center of gravity of the disk) in agreement with the result of operating without balls. The angular velocity of the disk, ω, was considered constant.

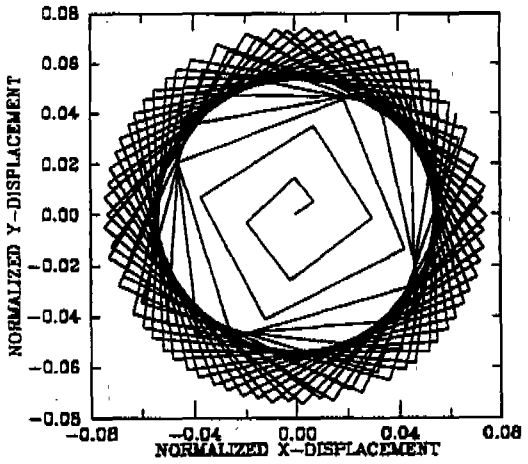

Fig. 8 X vs. Y direction displacement of the rotating system without balls at the first critical speed (Run conditions: ω/ω_n=1.0)

4. Operating at Critical Speed

Figures 7 to 12 show results of computer simulations at the critical speed. Figure 7 and 8 are plots of the motion of an unbalanced system containing no balls. The straight line

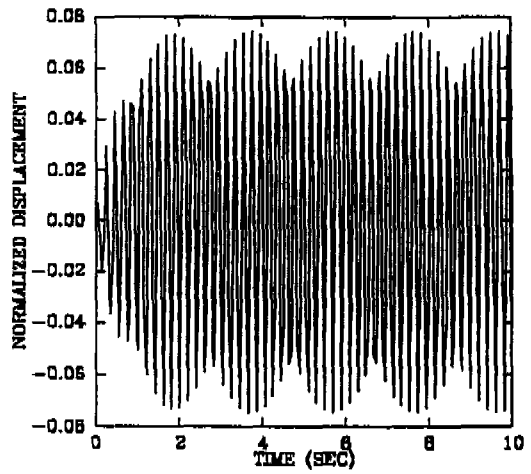

Fig. 7 Normalized displacement of the rotating system without balls at the first critical speed (Run conditions: ω/ω_n=1.0)

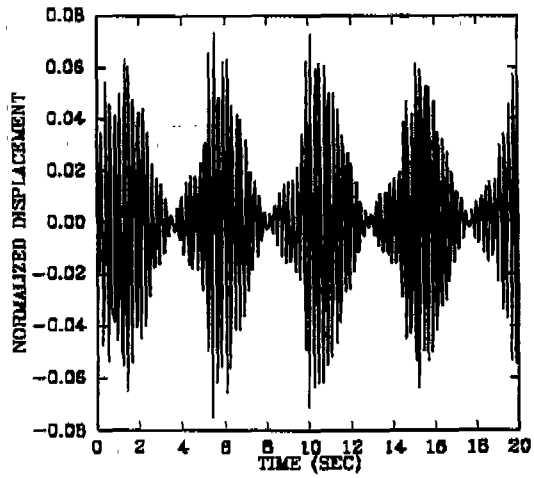

Fig. 9 Normalized displacement of the rotating system at the first critical speed (Run conditions: m/M = .005, ϵ/R=.001, β=2, and ω/ω_n=1.0)

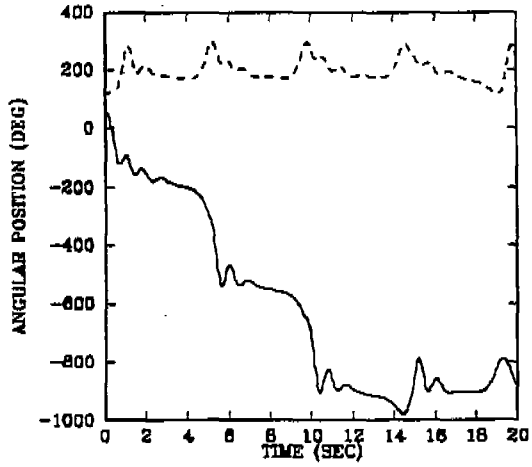

Fig. 10 Angular position of the two balls at the first critical speed(Run conditions: m/M = .005, ε/R=.001, β=2, $\phi_1(0)$=57, $\phi_2(0)$=115, and ω/ω_n=1.0)

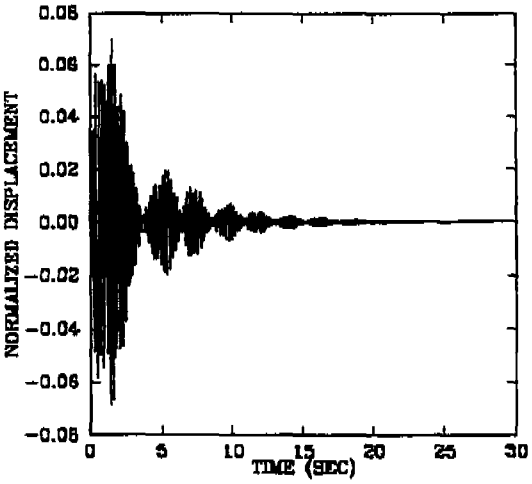

Fig. 11 Normalized displacement of the rotating system at the first critical speed(Run conditions:m/M = .005, ε/R=.001, β=5, and ω/ω_n= 1.0)

segments in Fig. 8 result from the time interval that was chosen. If the time step decreased, the shape will be changed to circle. This figure illustrates that with no balls, the rotating system vibrates with a constant amplitude after the transient decayed. The angular velocity of the disk was considered as

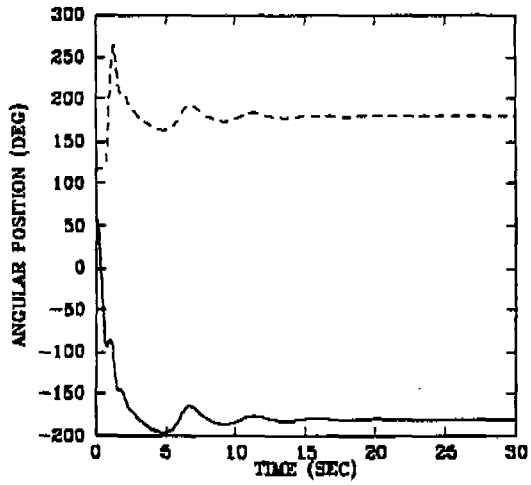

Fig. 12 Angular position of the two balls at the first critical speed(Run conditions:m/M = .005, ε/R=.001, β=5, $\phi_1(0)$=57, $\phi_2(0)$=115, and ω/ω_n=1.0)

a constant. Fig. 9 is a plot of the normalized displacement of the system, X/R, with two balls at critical speed. In this figure, the ratating system is not balanced by the two balls. Fig. 10 is a plot of angular position of the two balls at the first critical speed for β = 2, Fig. 10 shows that one of the two balls rotates around the race of SCDB with some angular velocity. Note that in these simulation the balls can pass each other. Fig. 11 and 12 show that increasing the damping coefficient, β, to 5, makes the system balance. Fig. 12 illustrates that when the rotating system operates at critical speed with larger viscous damping, the two steel balls are approximately positioned at 180 degrees. In this case large viscous damping can balance the system.

5. Operating below Critical Speed

Fig.s 13 to 18 show results of computer simulations below the critical speed. The angular velocity of the disk is considered as a con-

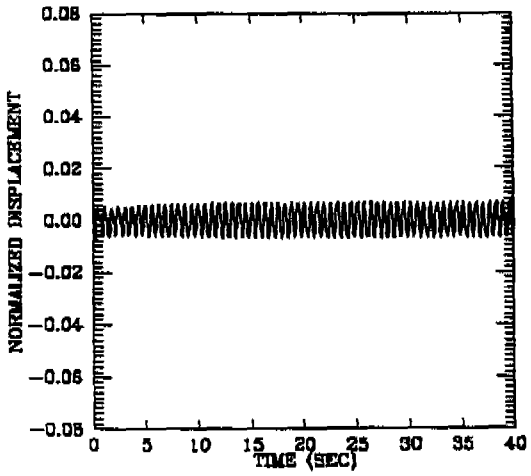

Fig. 13 Normalized displacement of the rotating system below the first critical speed(Run conditions: m/M = .005, ε/R=.001, β=2, and ω/ω_n=.7)

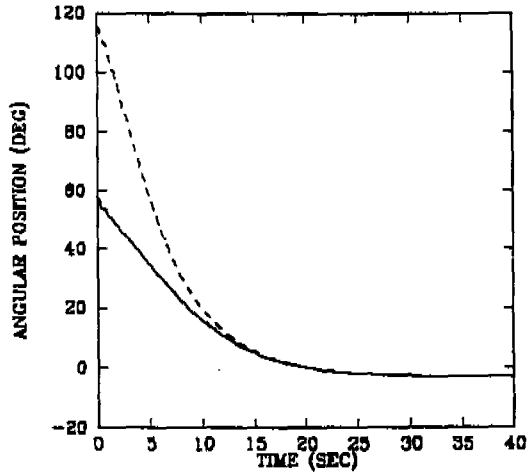

Fig. 14 Angular position of the two balls below the first critical speed(Run conditions:m/M = .005, ε/R=.001,β=2, $\phi_1(0)$=57, $\phi_2(0)$=115, and ω/ω_n=·7)

stant. Fig. 13 is a plot of the normalized displacement, X/R, of the system with two balls. Fig. 14 is a plot of the angular position of the two balls below the critical speed. This figure illustrates that when the rotating system operates below the critical speed the two steel balls are approximately positioned at zero degrees. This means that the two balls move toward the center of gravity side of the disk. In this case the two balls can not balance the system. To invesitigate stability of the system, different initial conditions, 174 and 186

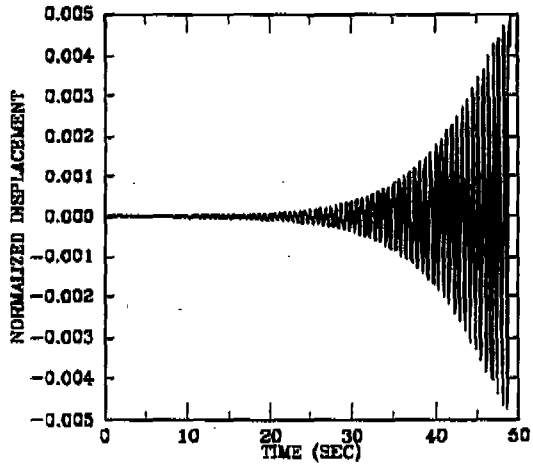

Fig. 15 Normalized displacement of the rotating system below the first critical speed(Run conditions:m/M = .005, ε/R=.001, β=2, $\phi_1(0)$=174, $\phi_2(0)$=186, and ω/ω_n=·7)

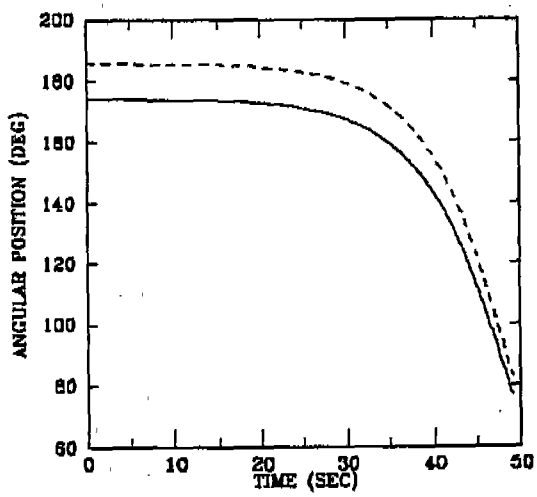

Fig. 16 Angular position of the two balls below the first critical speed(Run conditions: m/M = .005, ε/R=.001, β=2, $\phi_1(0)$= 174, $\phi_2(0)$=186 and ω/ω_n=·7)

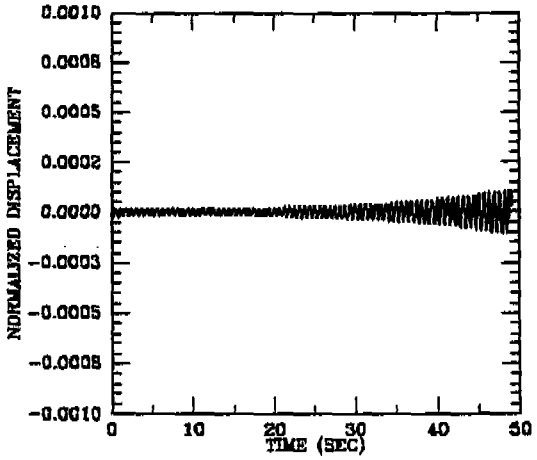

Fig. 17 Normalized displacement of the rotating system below the first critical speed (Run conditions: m/M = .005, ε/R=.001, β=5, $\phi_1(0)$=174, $\phi_2(0)$=186 and ω/ω_n= · 7)

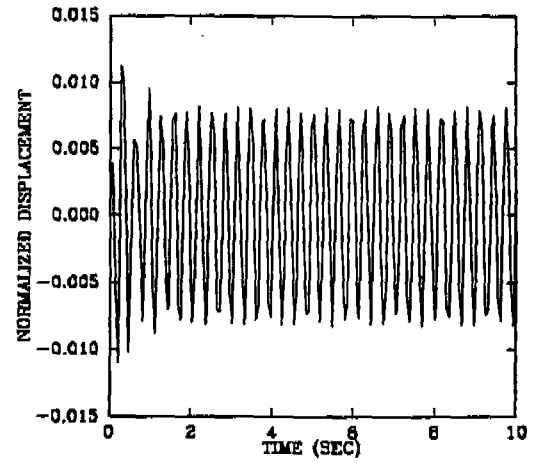

Fig. 18 Normalized displacement of the rotating system without balls below the first critical speed (Run conditions: ω/ω_n= · 7)

degree (these two initial positions can balance the system), are considered. The results are shown in Fig. 15 and 16. Below critical speed, Fig. 15 shows that even if the balls initially balance the system they do not remain in that position. With larger damping coefficient (β = 5), Fig. 17, the amplitude of the system is reduced compared to the case of β = 2. Fig. 18 shows a plot of the normalized displacement of the system with no balls.

6. Conclusions

In the limited computer simulations that have been presently carried out, several conclusions have been found. Above critical speed, the balls can balance the rotating disk with small damping between ball and race. At critical speed, the equilibrium of the system is depend on damping coefficient β. Large damping can balance the system. Below critical speed, the balls do not balance the system in any case.

To be credible, the SCDB must have, in addition to numerical appeal, demonstrated practical appeal. For a long, slender body, and non-uniform shaft, the dynamic unbalance cannot be compensated for by a single SCDB. Further study of this Self-Compensatins Dynamic Balancer for a nonuniform rotating system with variable rotating speed and the effect of β on stability for multiple balls should be done in the future.

REFERENCES

1. Jongkil Lee, "An Investigation of Dynamic Stability of Self-Compensating Dynamic Balancer," The Proceedings of the 64th Shock and Vibration Symposium, 1993
2. Alexander, J.D., "An Automatic Dynamic Balancer," The Proceedings of the 2nd Southeastern Conference, pp. 415-426, 1964
3. Cade, J.W., "Self-Compensating Balancing in Rotating Mechanisms," Design News, pp. 234-239, 1965
4. Darlow, M.S., Balancing of High-Speed Machinery, Springer-Verlag, New York,

1989

5. Rieger, N.F., Balancing of Rigid and Flexible Rotors, The Shock and Vibration Information Center, U.S. Department of Defense, 1986